Correlation time diffusion MRI: comparison to pulsed field gradient diffusion in brain imaging as a function of age

Hernan Jara[1], Stephan William Anderson[1], Jorge A Soto[1], and Osamu Sakai[1]

[1]Radiology, Boston University Medical Center, Boston, Massachusetts, United States

Purpose: Magnetic resonance-derived diffusion coefficients are almost exclusively generated by diffusion-weighting (DW) using pulsed-field gradient (PFG) pulse sequences. Nevertheless, *in vivo* PFG diffusion imaging remains challenging primarily because of its sensitivity to nondiffusive motions and concomitant T_2-weighting with resultant low SNR secondary to the relatively long minimum echo times. As an alternative to PFG diffusion imaging, tissue diffusion coefficients can be estimated by processing relaxometry data with quantum mechanical NMR relaxation theory. Because such diffusion techniques involve calculating the MR correlation time in an intermediate step, these will be referred to herein as correlation time diffusion (DCT) techniques. In this work, a DCT mapping algorithm that incorporates the three main phenomena affecting T_1 relaxation in tissue, specifically molecular kinetics, paramagnetic effects, and MT effects is applied experimentally to a variable sucrose concentration aqueous phantom as well as normal human brains and compared to standard PFG techniques. Because the relaxation times of brain tissues are functions of age (1), for this proof-of-concept work, we studied eleven subjects of different ages.

Methods: This study protocol was approved by the institutional review board of our institution; all subjects were consented following HIPAA guidelines. All imaging was performed on a 1.5 Tesla clinical MRI scanner (Intera, Philips Medical Systems of North America, Cleveland, OH, USA). The quadrature head coil was employed for both sucrose phantom and human brain imaging. The sucrose phantom consisted of vials of varying concentrations (3.914M, 2.921M, 1.928M, 1.169M, 0.660M, 0.345M, and 0.175M) of biochemistry-grade sucrose in 8MΩ solvent distilled water. The human subject study population consisted of 11 healthy research subjects (5 male, 6 female; aged 0.5-72.5 years). Images were acquired using the mixed turbo spin-echo (mixed-TSE) pulse sequence and two different DW PFG pulse sequences: single-slice DW conventional spin-echo (DW-CSE) for the phantom experiments and multi-slice single-shot echoplanar imaging (DW-SE-sshEPI) for brain imaging. Key imaging parameters for the mixed-TSE sequence: voxel dimensions=0.94x1.25x3.00mm, 80 contiguous slices, TR=14.88s, $TE1/2_{eff}$=7.1/100ms, TI1/2=700ms/7.44s, acquisition time=9:00min. Key imaging parameters for the DW-CSE sequence: voxel dimensions=0.94x1.05x5.00mm, single slice, TE=104ms, TR=1868, b-factors=0/800/1600, acquisition time=6:30min. Key imaging parameters for the DW-SE-sshEPI sequence: voxel dimensions=2.2x3.2x5.00mm, 25 slices, TE=74, b-factors=0/1000, acquisition time=1:00min. Mixed-TSE is a fast four time-points pulse sequence that combines in a single acquisition the principles of T_1-weighting by inversion recovery and of T_2-weighting by dual turbo spin echo sampling. This yields parametric maps of PD, T_1, and T_2 which are used as input to a series of equations incorporating the effects of molecular kinetics, paramagnetic and MT effects on T_1 relaxation time, ultimately yielding the rotational correlation time which is used to solve for the correlation time diffusion coefficient on a pixel by pixel basis.

Results: Typical correlation time diffusion coefficient maps are compared to slice-matched PFG maps in Figure 1. Visually, maps generated with the two diffusion techniques are similar at each level in terms of contrast appearance. DCT maps differ primarily in terms of lack of geometric deformation artifacts near the sinuses due to B0 inhomogeneities, which are typical of EPI sequences particularly with long echo trains. In addition, spatial resolution and SNR are improved in the case of the DCT, reflecting the underlying mixed-TSE acquisition. The visual appearance of the DCT and DPFG maps were similar for all subjects studied. For quantitative comparisons between the two diffusion techniques, the brain of each subject was segmented using dual clustering algorithms. After segmentation, whole-brain histograms of DCT and DPFG were generated and peaks were plotted demonstrating excellent linear correlation (slope=1.055, intercept=-0.041, and
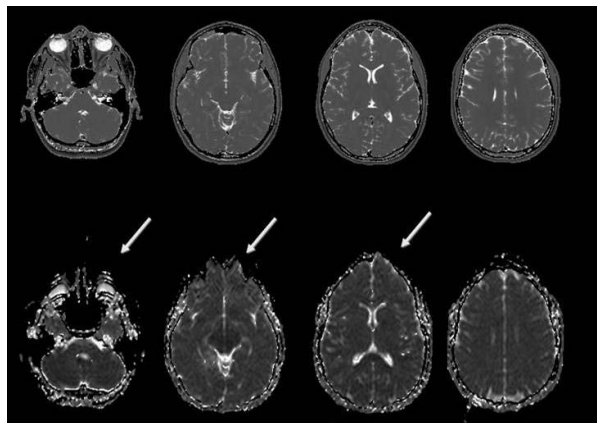

Figure 1. Comparison of DCT and DPFG maps. The differences relate to geometrical deformations (see arrows), which are typical of DPFG maps as well as improved spatial resolution and SNR in the case of the DCT maps.
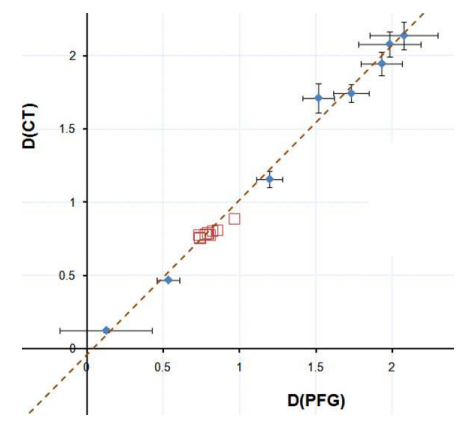

Figure 2. Plot of DPFG and DCT data (phantom and brains, brain=red boxes, sucrose solutions=blue circles). Linear regression analysis shows that the two diffusion coefficients are highly correlated (R^2=0.991) across a wide range of values.

R^2=0.991) between the DCT and DPFG data for the brain tissue as well as the sucrose aqueous solutions, which cover a much larger diffusion coefficient range than the brain data (Figure 2). The DCT and DPFG brain data show similar age related tendencies with overlapping histograms, as shown in Figure 3, over the age range studied. Notably, the histogram overlap of the youngest subject is poorer in comparison to the other subjects. Since the degree of myelination and consequently the level of magnetization transfer increase from birth to late adolescence, we tested the hypothesis that the DCT-DPFG discrepancy of the 0.5 year old subject could be reduced by adjusting the magnetization transfer coupling constant in the DCT algorithm (2). To this end, the DCT mapping algorithm was run in the approximation of null magnetization transfer effect, leading to a near perfect DCT-DPFG histogram agreement. Although this preliminary result suggests that the MT effects could be age dependent, additional experimentation would be needed to clarify this matter.

Conclusion: In this work, a correlation time diffusion (D_{CT}) MRI theoretical framework that incorporates the effects of molecular kinetics, paramagnetic solutes, and MT effects has been experimentally validated using a variable sucrose concentration aqueous phantom as well human brains over a range of ages. CTD diffusion MRI, overcoming several fundamental limitations of PFG techniques, may be useful for tissue characterization and for quantifying changes caused by disease.

Figure 3. Similar age related effects with the exception of the youngest subject 0.5 years old infant. Insert T_1 maps exemplify the very different levels of myelination between the 0.5 and the 17 year old subjects.

References: 1. Hasan KM, Walimuni IS, Kramer LA, Frye RE. Human brain atlas based volumetry and relaxometry: Application to healthy development and natural aging. Magn Reson Med. 2010;64(5):1382-1389.
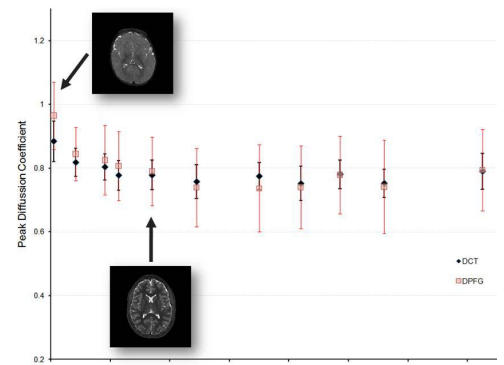2. Lebel C, Beaulieu C. Longitudinal development of human brain wiring continues from childhood into adulthood. J Neurosci. 2011;31(30):10937-10947.